Hsa_circ_0000670 regulates cell growth, angiogenesis and glutamine metabolism of gastric cancer cells through miR-141-3p/ALKBH1 axis

Jiajun Lu
The First Hospital of Jiaxing, The Affiliated Hospital of Jiaxing University
Yuan Zhou
The First Hospital of Jiaxing, The Affiliated Hospital of Jiaxing University
Zhiheng Chen
The First Hospital of Jiaxing, The Affiliated Hospital of Jiaxing University
Honggang Jiang
The First Hospital of Jiaxing, The Affiliated Hospital of Jiaxing University
Jin Li
The First Hospital of Jiaxing, The Affiliated Hospital of Jiaxing University
Guangjian Dou (pvag9rh@163.com)
The First Hospital of Jiaxing, The Affiliated Hospital of Jiaxing University

Research Article

Keywords: circ_0000670, miR-141-3p, ALKBH1, gastric cancer

Posted Date: June 23rd, 2022

DOI: https://doi.org/10.21203/rs.3.rs-1770145/v1

Abstract

Background: Gastric cancer (GC) is one of the four most deadly tumors in the world, and its occurrence is influenced by genetic and environmental factors. CircRNA-miRNA-mRNA is reported to be associated with variety cancer, including GC.

Methods: The expression of hsa_circ_0000670, miR-141-3p and AlkB homolog 1 (ALKBH1) were detected by quantitative real-time polymerase chain reaction (qRT-PCR). Cell proliferation and apoptosis were detected by 5-Ethynyl-2'-deoxyuridine (EdU) assay and flow cytometry. The protein expression levels were measured by western blot and immunohistochemistry (IHC). Tube forming experiment was performed to assess angiogenesis rate. The levels of glutamine and α-ketoglutaric acid (α-KG) were examined using commercial kits. The target interaction between miR-141-3p and circ_0000670 or ALKBH1 was verified by dual-luciferase reporter assay and RNA immunoprecipitation (RIP) assay. The effect of circ_0000670 on tumor *in vivo* was analyzed in mice.

Results: Circ_0000670 had a stable ring structure and was accelerated in GC tissues and cells. The proliferation of GC was hampered by circ_0000670 knockdown *in vivo* and *in vitro*, and the apoptosis rate was increased by circ_0000670 knockdown. Circ_0000670 down-regulation suppressed angiogenesis, the level of glutamine and α-KG in GC cells. The impacts of circ_0000670 knockdown on GC were relieved by miR-141-3p inhibition. The results indicated that circ_0000670 silencing could induce cell proliferation decline in GC, which was ameliorated by miR-141-3p knockdown. The functions of miR-141-3p mimic on cell proliferation, apoptosis, angiogenesis, glutamine and α-KG were reversed by ALKBH1 up-regulation.

Conclusion: Our findings revealed that circ_0000670 promoted GC progression though miR-141-3p and ALKBH1, suggesting that circ_0000670 might be a target for GC clinical treatment.

Highlights

1. Hsa_circ_0000670 promoted GC growth *in vitro* and *in vivo*.
2. ALKBH1 was co-regulated by circ_0000670 and miR-141-3p in GC cells.
3. MiR-141-3p inhibitor abolished the effects of circ_0000670 knockdown on GC progression.
4. The effects of miR-141-3p mimic in GC cells were receded after ALKBH1 overexpression.

1. Introduction

Gastric cancer (GC) is one of the fourth deadliest tumors entire world, and the survival rate in advanced stage is low[1]. The development of cancer is influenced by environmental factors such as eating habits and heredity[2]. Therefore, exploring the genetic mechanism of GC can provide molecular targets for clinical treatment of GC.

More and more researchers focus on the genetic mechanism of cancer occurrence. Molecular biology information technologies such as Gene Ontology analysis and Kyoto Encyclopedia of Genes and Genomes pathway are employed to analyze the function of circRNA-miRNA-RNA network in cancer development to identify molecular markers that can be effectively used in cancer treatment[3, 4]. Liu *et al.* confirmed that circWHSC1 was greatly boosted in endometrial cancer tissues, and that circWHSC1 sponged miR-646 and targeted nucleophosmin 1 (NPM1) to promote the proliferation, migration and invasion of endometrial cancer cells, and reduced cell apoptosis[5]. It is found that hsa_circ_0000670 could combine miR-384 to target SIX homeobox 4 (SIX4) and regulate the development of GC[6].

MiRNAs, as non-coding RNAs, can be sponged by circRNAs, and can also target mRNAs to regulate a variety of physiological activities in organisms[7]. Hsa_circ_001783 was highly expressed in breast cancer (BC) tissues and cells, and low expression of circ_001783 significantly confined the progression of BC cells, and the data of functional tests implied that hsa_circ_001783 acted as a sponge of miR-200c-3p and promoted the development of BC cells[8]. Increasing researches exhibited that miR-141-3p was involved in the occurrence and development of many diseases, like vascular smooth muscle cells (VSMCs)[9], necrotizing enterocolitis[10], nasopharyngeal carcinoma[11] and endometrial stromal[12]. MiR-141-3p was obviously reduced in the plasma of patients with GC[13], and might inhibit NF-kB pathway to restrain the proliferation and migration of human GC cells[14]. But, the interaction between miR-141-3p and circ_0000670 in GC is unclear.

AlkB homolog 1 (ALKBH1) is identified for the first time as an N^6-mA demethylase of local unpaired DNA[15], and is involved in the development of lung cancer[16], glioblastoma[17] and other diseases[18]. It's reported that the significant down-regulation of ALKBH1 in GC tissues was closely related to the larger tumor size and the later TNM stage[19]. However, the function of ALKBH1 in GC and the role of circ_0000670-miR-141-3p-ALKBH1 axis in GC have not been reported.

The mechanism of circ_0000670-miR-141-3p-ALKBH1 axis in GC was explored without precedent. The effect of circ_0000670 on glutamine metabolism in GC cells was demonstrated first time. This study opens up a new possibility for the clinic treatment and prognosis of GC patients.

2. Materials And Methods

2.1 Clinical specimens

Approved by the Ethics Committee of Department of Gastrointestinal Surgery, The First Hospital of Jiaxing, The Affiliated Hospital of Jiaxing University, forty-three patients with GC in Department of Gastrointestinal Surgery, The First Hospital of Jiaxing, The Affiliated Hospital of Jiaxing University voluntarily signed written consent forms and afforded their gastric tissues and adjacent tissues. When these tissues were isolated, they were immediately saved in liquid nitrogen until to use.

2.2 Cell lines and cell culture

Nanjing Kebai Biological Technology Co., Ltd (Nanjing, China) furnished the normal gastric epithelial cell line GES-1 and GC cell lines (AGS and HGC-27). All cells were hatched in RPMI-1640 (BIOSUN, Shanghai, China) with 10% fetal bovine serum (FBS; Bovogen, Melbourne, Australia) and 1% streptomycin-penicillin (HyClone Company, Logan, UT, USA) at 37°C with 5% CO_2.

2.3 Hematoxylin & eosin (H&E) staining assay

The paraffin sections from tumor tissues and normal tissues were dewaxed with xylene (Merck, Darmstadt, Germany) and gradually dehydrated with ethanol (Merck). Hematoxylin and Eosin Staining Kit (YEASEN, Shanghai, China) instructions were followed for staining. Sections were dehydrated with alchol and sealed and histological analysis with a microscope.

2.4 RNA extraction and quantitative real-time polymerase chain reaction (qRT-PCR)

The total RNA from cells or tissues was leached with TRIzol (Total RNA Extraction reagent) (Prilai Gene Technology Co., Ltd, Beijing, China). The RNA extracted was quantitatively analyzed using SYBR Green PCR Master Mix (Applied Biosystems, Foster City, CA, USA) in the Real-Time PCR Detection System (Bio-Rad, Shanghai, China). Housekeeping genes were glyceraldehyde 3-phosphate dehydrogenase (GAPDH) and small nuclear RNA U6 (U6). The primers used in this experiment (Table 1) were all synthesized in Suzhou Hongxun Biological Technology Co., Ltd (Suzhou, China).

Table 1
Sequences used for RT-qPCR

Name		Primers sequences for PCR (5'-3')
hsa_circ_0000670	Forward	TGCATTCTTACTCTTAGGGTTCA
	Reverse	TCATTTTCTTCCTAGACAAAGCCT
ALKBH1	Forward	CTTTGGACAGTCCGCCATCT
	Reverse	AACACGAGCGGTCTTCAAGT
miR-141-3p	Forward	GCCGAGTAACACTGTCTGGTAA
	Reverse	TGGTGTCGTGGAGTCG
C16orf72	Forward	TAAGCGTGCGTTCGAGTACC
	Reverse	TGTCCAAGTGGAGTGCCATT
GAPDH	Forward	AAGGCTGTGGGCAAGGTCATC
	Reverse	GCGTCAAAGGTGGAGGAGTGG
U6	Forward	CTCGCTTCGGCAGCACATA
	Reverse	CGAATTTGCGTGTCATCCT

2.5 RNase R assay

RNA was cultured with 100 μg/mL RNase R (Epicentre, Madison, Wisconsin, USA). Then, qRT-PCR was executed to monitor the levels of circ_0000670 and C16orf72, respectively.

2.6 Cell transfection

Small interfering (si)RNA of circ_0000670 (si-circ_0000670), siRNA negative control (si-NC), short hairpin (sh)RNA of circ_0000670 (sh-circ_0000670), shRNA NC (sh-NC), miR-141-3p mimic, miRNA NC, miR-141-3p inhibitor, inhibitor NC, ALKBH1 expressing plasmid in pcDNA vector (pc-ALKBH1), and pcDNA NC (pc-NC) were synthesized or purchased from Genepharma (Shanghai, China) and Sangon Biotech (Shanghai, China). Lipofectamine 2000 transfection reagent (Invitrogen, Carlsbad, California, USA) was used to perform transient transfection. Transfection efficiency was tested after transfection for 48 h.

2.7 5-Ethynyl-2’-deoxyuridine (EdU) assay

EdU assay was conducted using an EdU apollo 567 *in vitro* kit (Solarbio, Beijing, China). GC cells were seeded onto the confocal plates and were incubated with 50 μM EdU reagent for 2 h. Cell nucleus was stained with DAPI reagent (Sigma, St. Louis, MO, USA). Cell fluorescence images were captured using a fluorescence microscope (Olympus, Tokyo, Japan).

2.8 Cell apoptosis assay

An Annexin V-fluorescein isothiocyanate (FITC)/propidium iodide (PI) kit (BD Biosciences, Franklin Lakes, NJ, USA) was used to analyze the apoptosis of GC cells. AGS and HGC-27 cells were assembled after transfected with si-circ_0000670 or si-NC for 48 h, and cells were diluted and hatched with 5 μL Annexin V-FITC at 2–8℃ in the dark for 15 min. Then cells were fostered with 10 μL of PI solution at 2–8℃ for 5 min. Flow cytometry (Agilent, Beijing, China) was used to detect and photograph the apoptotic cells within 1 h.

2.9 Western blot

Proteins was leached from cells by Radio Immunoprecipitation Assay (RIPA) lysis buffer containing protease phosphatase inhibitors and Phenylmethanesulfonyl fluoride (PMSF) (Prilai Gene Technology Co., Ltd), and the concentration of protein was measured by protein quantification Kit (BCA method) (Prilai Gene Technology Co., Ltd). Proteins of different lengths were separated via SDS-PAGE Kit (Shanghai Guduo Biological Technology Co., Ltd, Shanghai, China). The polyvinylidene fluoride (PVDF) membrane (Millipore, Billerica, MA, USA) was engaged to shift the proteins, and was sealed with 5% albumin from chicken egg white (Solarbio) for 2 h. PVDF membrane was hatched with the primary antibodies at 4℃ overnight, including anti-Bcl-2 associated X, apoptosis regulator (anti-Bax; ab32503; 1:8000; Abcam, Cambridge, MA, USA), anti-B cell leukemia/lymphoma 2 (anti-Bcl-2; ab32124; 1:8000; Abcam), anti-ALKBH1 (ab126596; 1:5000; Abcam), and anti-GAPDH (ab8245; 1:20000; Abcam). Subsequently, the membrane was incubated with the horseradish peroxidase (HRP)-conjugated secondary antibodies (ab288151; 1:3000; Abcam) for 2 h at room temperature, added with ECL Plus

hypersensitive luminescence solution (Solarbio), and photographed in a gel imaging analyzer (UVITEC, Cambridge, England).

2.10 Angiogenesis Assay

10 μL of Matrigel (BD Biosciences) melted in a refrigerator at 4°C was added to sterile ibidi angiogenesis slide, and the slide was placed in a wet box for later use. A 50 μL si-NC or si-circ_0000670 cell suspension with the density of 2×10^5 cells/mL was added to the Matrigel gel well and the serum-free medium was added to the well for a period of time to induce angiogenesis. Tube formation was observed and photographed under a microscope (Olympus).

2.11 Glutamine metabolism assay

The effect of circ_0000670 on glutamine in AGS and HGC-27 cells was measured with Glutamine Assay Kit (Abcam). In brief, fresh medium and cell medium were mingled with enzyme and incubated in dark for a period of time, respectively, and the absorbance at 565 nm was detect. The level of α-Ketoglutaric acid (α-KG) in cells was assessed with a α-ketoglutaric acid (α-KG) Kit (Ruixin Biotechnology Co., Ltd, Fujian, China).

2.12 Dual-luciferase reporter assay

Circ_0000670 and ALKBH1 wild-type and mutant dual fluorescence reporter vectors (WT-circ_0000670, MUT-circ_0000670, WT-ALKBH1-3'UTR and MUT-ALKBH1-3'UTR) were co-transfected into AGS and HGC-27 cells with miR-141-3p mimic or miRNA NC, respectively. The luciferase activity of each groups was measured in a TD20/20 Luminometer (Turner Biosystems, Sunnyvale, CA, USA) according to the Double-luciferase reporter Gene Test Kit (Beyotime Biotechnology, Jiangsu, China) after transfected for 48 h.

2.13 RNA immunoprecipitation (RIP) assay

RIP experiments were performed to analyze the binding effects between miR-141-3p and circ_0000670 or ALKBH1. An equal volume of RIP lysis buffer (Millipore, Billerica, MA, USA) was appended to the AGS and HGC-27 cell precipitate to lyse cells to prepare cell suspensions. Then cell pellets were incubated with anti-Ago2 antibody (Abcam) or anti-IgG antibody (Abcam)-magnetic beads. Then the complex was cultivated with proteinase K (Thermo Fisher Scientific, Rockville, MD, USA) to remove proteins. The extracted RNA was isolated by TRNZOL reagent (TIANGEN, Beijing, China), and circ_0000670, miR-141-3p and ALKBH1 were quantified by qRT-PCR.

2.14 In vivo experiment

A total of six BALB/c nude mice (5 weeks old) from the Vital River Laboratory Animal Technology (Beijing, China) were divided into two groups at random, one group was inoculated with HGC-27 cells transfected with sh-NC as a control group and the other group was inoculated with HGC-27 cells transfected with sh-circ_0000670. The size of tumor was measured every weeks as length×width^2×0.5, and the mice were

killed painlessly after the size of tumor was measured on the fourth weeks, and the mass of tumors were weighed. These animal experiments were approved by the Animal Welfare and Research Ethics Committee of Department of Gastrointestinal Surgery, The First Hospital of Jiaxing, The Affiliated Hospital of Jiaxing University.

2.15 Immunohistochemistry (IHC) assay

The protein expression of marker of proliferation Ki-67 (MKI67, Ki67) was detected by IHC. Tumor tissues of mice in sh-circ_0000670 group and sh-NC group were made into tissue sections with formalin and paraffin, and the slices were treated with Ki-67 antibody (ab15580; 1:300; Abcam) and the secondary antibody (ab288151; 1:500; Abcam). The samples were dyed with diaminobenzidine (Sangon Biotech) and the expression of Ki67 was assessed according to the integrated optical density in each stained area.

2.16 Statistical analysis

SPSS 21.0 (SPSS, Chicago, Illinois, USA) and GraphPad Prism 8.0 software (GraphPad Inc., LaJolla, California, USA) were serviced for data analysis and graphs. The Student's *t*-test and analysis of variance (ANOVA) were employed for comparisons in data. Results were presented as "mean ± standard deviation", and $P < 0.05$ was thought statistically significant.

3. Results

3.1 Circ_0000670 was up-regulated in GC tissues and cells

We first identified GC tissue samples and adjacent normal tissue samples with H&E (Fig. 1A). Then we explored the abundance of circ_0000670 in GC tissues and cells with qRT-PCR. As illustrated in Fig. 1B, a significantly upregulated circ_0000670 level was observed in GC tissues compared with adjacent normal tissues. Circ_0000670 expression was also up-regulated in two GC cell lines (AGS and HGC-27) compared with a normal gastric epithelial cell line GES-1 (Fig. 1C). RNase R assay exhibited that circ_0000670 was more stable than C16orf72 in AGS and HGC-27 cells because of its ring structure (Fig. 1D-E). In short, circ_0000670 was up-regulated in GC tissues and cells, which might be a molecular target of GC.

3.2 Circ_0000670 interference inhibited GC cell growth

Firstly, the transfection efficiency of si-circ_0000670 was tested via qRT-PCR. Circ_0000670 expression was dramatically inhibited in AGS and HGC-27 cells after transfected with si-circ_0000670 (Fig. 2A). Circ_0000670 knockdown reduced the percentage of EdU-positive GC cells (Fig. 2B), suggesting that circ_0000670 silencing suppressed the proliferation of GC cells. Apoptosis rate of AGS and HGC-27 cells was obviously increased with the silencing of circ_0000670 (Fig. 2C). Si-circ_0000670 increased the protein expression of Bax in AGS and HGC-27 cells, and inhibited the expression of Bcl-2 in AGS and HGC-27 cells (Fig. 2D-E). Angiogenesis assay showed that the tube formation in AGS and HGC-27 cells was markedly reduced in si-circ_0000670 group (Fig. 2F). After AGS and HGC-27 cells were transfected with si-

circ_0000670, glutamine and α-KG in AGS and HGC-27 cells were remarkably restrained (Fig. 2G-H). Taken together, circ_0000670 played an oncogenic role in GC cells *in vitro*.

3.3 MiR-141-3p was decreased in GC and was regulated by circ_0000670

For the sake of probing the mechanism of circ_0000670, circBanK (http://www.circbank.cn) was used to seek for miRNAs that might interact with circ_0000670. We found that circ_0000670 might serve as a molecule sponge for miR-141-3p (Fig. 3A). Compared with miRNA NC group, the expression of miR-141-3p in AGS and HGC-27 cells was strikingly increased in miR-141-3p mimic group (Fig. 3B). Compared with miRNA NC, miR-141-3p inhibited the luciferase activity of WT-circ_0000670, while it had no effect on luciferase activity of MUT-circ_0000670 (Fig. 3C-D). Moreover, RIP assay results indicated that both circ_0000670 and miR-141-3p were markedly enriched by Ago2 (Fig. 3E-F). MiR-141-3p was conspicuously constrained in GC tissues and cells (Fig. 3G-H). And miR-141-3p was notably boosted in AGS and HGC-27 cells transfected with si-circ_0000670 than that in the control group (Fig. 3I). The data suggested circ_0000670 negatively regulated miR-141-3p in GC cells.

3.4 The effects of circ_0000670 knockdown on the biological behaviors of GC cells were overturned by anti-miR-141-3p

MiR-141-3p inhibitor suppressed the miR-141-3p expression in cells (Fig. 4A). MiR-141-3p silencing reverted the impacts of circ_0000670 depletion on proliferation and apoptosis of AGS and HGC-27 cells (Fig. 4B-C). Bax was boosted by si-circ_0000670, while Bcl-2 was hindered by si-circ_0000670, and these affects were restored by miR-141-3p inhibitor (Fig. 4D-E). MiR-141-3p inhibition reversed the decrease of angiogenesis, glutamine consumption and α-KG production in circ_0000670-silenced AGS and HGC-27 cells (Fig. 4F-H). The data proved that si-circ_0000670-mediated effects on the biological behaviors of GC cells were reversed by miR-141-3p down-regulation.

3.5 ALKBH1 was targeted by miR-141-3p in GC cells

Starbase (http://starbase.sysu.edu.cn) was used to predict the target gene of miR-141-3p, as shown in Fig. 5A, there was a binding site for miR-141-3p in the 3'UTR region of ALKBH1. We observed that miR-141-3p overexpression repressed the luciferase activity in AGS and HGC-27 cells carrying the luciferase plasmid containing WT-ALKBH1-3′UTR but not the luciferase plasmid containing MUT-ALKBH1-3′UTR (Fig. 5B-C). The data of RIP assay indicated that miR-141-3p and ALKBH1 were markedly enriched in the Ago2 group (Fig. 5D-E). ALKBH1 was distinctly boosted in GC tissues and cells, and negatively regulated by miR-141-3p (Fig. 5F-I). Restoration experiments displayed the inhibitory effect of si-circ_0000670 on ALKBH1 was reversed after miR-141-3p inhibitor co-transfection (Fig. 5J). In a word, ALKBH1 was up-regulated in GC tissues and cells, and regulated by circ_0000670 and miR-141-3p.

3.6 ALKBH1 overexpression reversed the effects of miR-141-3p overexpression on GC cells

The transfection efficiency of pc-ALKBH1 in AGS and HGC-27 cells was measured by western blot, the result manifested the expression of ALKBH1 was obviously enhanced (Fig. 6A). The inhibitory effect of miR-141-3p mimic on cell proliferation was regained in AGS and HGC-27 cells co-transfected with pc-ALKBH1 (Fig. 6B). MiR-141-3p mimic promoted apoptosis in AGS and HGC-27 cells, while pc-ALKBH1 alleviated this effect (Fig. 6C). The expression of Bax was increased, while Bcl-2 was hampered in GC cells with miR-141-3p mimic transfection, and ALKBH1 overexpression reversed these effects (Fig. 6D-E). ALKBH1 overexpression rescued the angiogenesis and glutamine metabolism in miR-141-3p-overexpressed GC cells (Fig. 6F-H). In brief, the effects of miR-141-3p mimic on GC cells was reverted by ALKBH1 overexpression.

3.7 Circ_0000670 knockdown inhibited the growth of GC *in vivo*

Mouse tumor model was constructed to analyze the effects of circ_0000670 on GC *in vivo*. Tumor volume and weight were greatly curbed in sh-circ_0000670 group than sh-NC group (Fig. 7A-B). We revealed that after injection of sh-circ_0000670-transfected HGC-27 cells into mice, circ_0000670 expression in tissues was significantly reduced (Fig. 7C). The expression of miR-141-3p was elevated while ALKBH1 was decreased in sh-circ_0000670 group (Fig. 7D-E). The data of immunohistochemical assay demonstrated that the protein level of Ki67 was reduced in the lower circ_0000670 expression group (Fig. 7F).

4. Discussion

GC is the second deadliest malignant tumor in human, ten million new cases of GC were reported in 2018[20]. CircRNAs have been certified to be involved in GC therapy as oncogenes or tumor suppressor genes[21–23]. Yang[24] *et al.* showed that circ-HUR inhibited the progression of GC by down-regulating the expression of HuR gene though binding to CNBP. The overexpression of circ-DONSON in GC promoted the growth of GC cells, and circ-DONSON was associated with Tumor Node Metastasis (TNM) stage and poor prognosis in GC patients[25]. Circ_0110805 could inhibit the expression of ENDOPDI by miR-299-3p to inhibit the cisplatin sensitivity and apoptosis of GC cells[26]. In our study, we presented that circ_0000670 was markedly aggrandized in GC tissues and cells, and the results of function experiment displayed that silencing circ_0000670 remarkably suppressed cell proliferation and accelerated cell apoptosis *in vitro*, and impeded tumor growth *in vivo*, which was consistent with the findings of Yang[6] *et al*. We also found that silence of circ_0000670 strikingly facilitated the level of Bax, while evidently restrained the level of Bcl-2 in GC cells. Besides, we data suggested that circ_0000670 knockdown obviously hindered angiogenesis, glutamine metabolism of GC cells. In a word, down-regulation of circ_0000670 might inhibit cell proliferation by inhibiting glutamine metabolism in GC.

CircBank was used to predict that miR-141-3p was the target gene of circ_0000670, and which was verified by dual-luciferase reporter experiment and RIP assay. The data discovered that miR-141-3p was diminished in GC tissues and cells, and the proliferation of GC cells *in vitro* was blocked with miR-141-3p overexpression. Similarly, Liu[27] *et al.* found that the abilities of GC cells to migrate and invade were confined with miR-141-3p mimic transfection, and miR-141-3p retarded cell viability. We also implied that the level of Bax was augmented with miR-141-3p up-regulation, and the levels of Bcl-2, angiogenesis, glutamine metabolism of GC cells were impeded with miR-141-3p overexpression. The data in our study indicated the effects of si-circ_0000670 on proliferation, apoptosis, Bax, Bcl-2, angiogenesis, glutamine metabolism were reversed in GC cells co-transfected with miR-141-3p inhibitor. In short, circ_0000670 could regulate the development of GC by sponging miR-141-3p.

ALKBH1 was predicted and confirmed to be a target gene of miR-141-3p via Starbase, dual-luciferase reporter experiment and RIP assay in the study. The data disclosed that ALKBH1 in GC tissues and cells was specially enhanced, and was passively controlled by miR-141-3p. Wang[28] *et al.* also elucidated that ALKBH1 was pronouncedly reinforced in GC tissues. Besides, we found that miR-141-3p deficiency reversed the inhibitory effect of circ_0000670 knockdown on ALKBH1 in GC cells. And the effects of miR-141-3p mimic on GC cells were recuperated after ALKBH1 overexpression. In a word, circ_0000670 regulated cell growth though miR-141-3p/ALKBH1 axis in GC.

5. Conclusion

In this study, we found that circ_0000670 was fortified in GC tissues and cells, and it was an oncogene in GC. Circ_0000670 promoted the progression of GC by increasing glutamine metabolism through the miR-141-3p/ALKBH1 axis.

Declarations

Acknowledgements

Disclosure of interest

The authors declare that they have no conflicts of interest.

Funding

This work was supported by **Jiaxing City Science and Technology Plan Project（No.2019AD32262）**

References

1. Zhang XY, Zhang PY. Gastric cancer: somatic genetics as a guide to therapy. Journal of medical genetics. 2017;54(5):305–312.

2. Machlowska J, Baj J. Gastric Cancer: Epidemiology, Risk Factors, Classification, Genomic Characteristics and Treatment Strategies. 2020;21(11).
3. Tian Y, Xing Y, Zhang Z. Bioinformatics Analysis of Key Genes and circRNA-miRNA-mRNA Regulatory Network in Gastric Cancer. 2020;2020:2862701.
4. Yang G, Zhang Y, Yang J. Identification of Potentially Functional CircRNA-miRNA-mRNA Regulatory Network in Gastric Carcinoma using Bioinformatics Analysis. Medical science monitor: international medical journal of experimental and clinical research. 2019;25:8777–8796.
5. Liu Y, Chen S, Zong ZH, et al. CircRNA WHSC1 targets the miR-646/NPM1 pathway to promote the development of endometrial cancer. 2020;24(12):6898–6907.
6. Liu P, Cai S, Li N. Circular RNA-hsa-circ-0000670 promotes gastric cancer progression through the microRNA-384/SIX4 axis. Experimental cell research. 2020;394(2):112141.
7. Cheng Y, Su Y, Wang S, et al. Identification of circRNA-lncRNA-miRNA-mRNA Competitive Endogenous RNA Network as Novel Prognostic Markers for Acute Myeloid Leukemia. 2020;11(8).
8. Liu Z, Zhou Y. Circular RNA hsa_circ_001783 regulates breast cancer progression via sponging miR-200c-3p. 2019;10(2):55.
9. Zhang X, Li H, Guo X, et al. Long Noncoding RNA Hypoxia-Inducible Factor-1 Alpha-Antisense RNA 1 Regulates Vascular Smooth Muscle Cells to Promote the Development of Thoracic Aortic Aneurysm by Modulating Apoptotic Protease-Activating Factor 1 and Targeting let-7g. The Journal of surgical research. 2020;255:602–611.
10. Li X, Wang Y, Wang Y, et al. MiR-141-3p ameliorates RIPK1-mediated necroptosis of intestinal epithelial cells in necrotizing enterocolitis. Aging. 2020;12(18):18073–18083.
11. Li M, Huang H, Cheng F, et al. miR-141-3p promotes proliferation and metastasis of nasopharyngeal carcinoma by targeting NME1. Advances in medical sciences. 2020;65(2):252–258.
12. Zhang Y, Yan J, Pan X. miR-141-3p affects apoptosis and migration of endometrial stromal cells by targeting KLF-12. Pflugers Archiv: European journal of physiology. 2019;471(8):1055–1063.
13. Ghaedi H, Mozaffari MAN, Salehi Z, et al. Co-expression profiling of plasma miRNAs and long noncoding RNAs in gastric cancer patients. Gene. 2019;687:135–142.
14. Wang F, Yang JX, Chen ZN. [Effects of miR-141-3p on proliferation, migration and NF-κB signaling pathways in gastric cancer cells]. Zhonghua zhong liu za zhi [Chinese journal of oncology]. 2020;42(7):556–559.
15. Zhang M, Yang S, Nelakanti R, et al. Mammalian ALKBH1 serves as an N(6)-mA demethylase of unpairing DNA. 2020;30(3):197–210.
16. Li H, Zhang Y, Guo Y, et al. ALKBH1 promotes lung cancer by regulating m6A RNA demethylation. Biochemical pharmacology. 2021;189:114284.
17. Xie Q, Wu TP, Gimple RC, et al. N(6)-methyladenine DNA Modification in Glioblastoma. Cell. 2018;175(5):1228–1243.e1220.

18. Zhang Y, Wang C. Demethyltransferase AlkBH1 substrate diversity and relationship to human diseases. 2021;48(5):4747–4756.
19. Li Y, Zheng D, Wang F, et al. Expression of Demethylase Genes, FTO and ALKBH1, Is Associated with Prognosis of Gastric Cancer. Digestive diseases and sciences. 2019;64(6):1503–1513.
20. Bray F, Ferlay J, Soerjomataram I, et al. Global cancer statistics 2018: GLOBOCAN estimates of incidence and mortality worldwide for 36 cancers in 185 countries. CA: a cancer journal for clinicians. 2018;68(6):394–424.
21. Li R, Jiang J, Shi H, et al. CircRNA: a rising star in gastric cancer. Cellular and molecular life sciences: CMLS. 2020;77(9):1661–1680.
22. Zhang X, Wang S, Wang H, et al. Circular RNA circNRIP1 acts as a microRNA-149-5p sponge to promote gastric cancer progression via the AKT1/mTOR pathway. Molecular cancer. 2019;18(1):20.
23. Zhang Y, Liu H, Li W, et al. CircRNA_100269 is downregulated in gastric cancer and suppresses tumor cell growth by targeting miR-630. Aging. 2017;9(6):1585–1594.
24. Yang F, Hu A, Li D, et al. Circ-HuR suppresses HuR expression and gastric cancer progression by inhibiting CNBP transactivation. 2019;18(1):158.
25. Ding L, Zhao Y, Dang S, et al. Circular RNA circ-DONSON facilitates gastric cancer growth and invasion via NURF complex dependent activation of transcription factor SOX4. 2019;18(1):45.
26. Yang X, Zhang Q, Guan B. Circ_0110805 Knockdown Enhances Cisplatin Sensitivity and Inhibits Gastric Cancer Progression by miR-299-3p/ENDOPDI Axis. OncoTargets and therapy. 2020;13:11445–11457.
27. Liu Y, Lin W, Dong Y, et al. Long noncoding RNA HCG18 up-regulates the expression of WIPF1 and YAP/TAZ by inhibiting miR-141-3p in gastric cancer. Cancer medicine. 2020;9(18):6752–6765.
28. Wang C, Huang Y, Zhang J, et al. MiRNA-339-5p suppresses the malignant development of gastric cancer via targeting ALKBH1. Experimental and molecular pathology. 2020;115:104449.

Figures

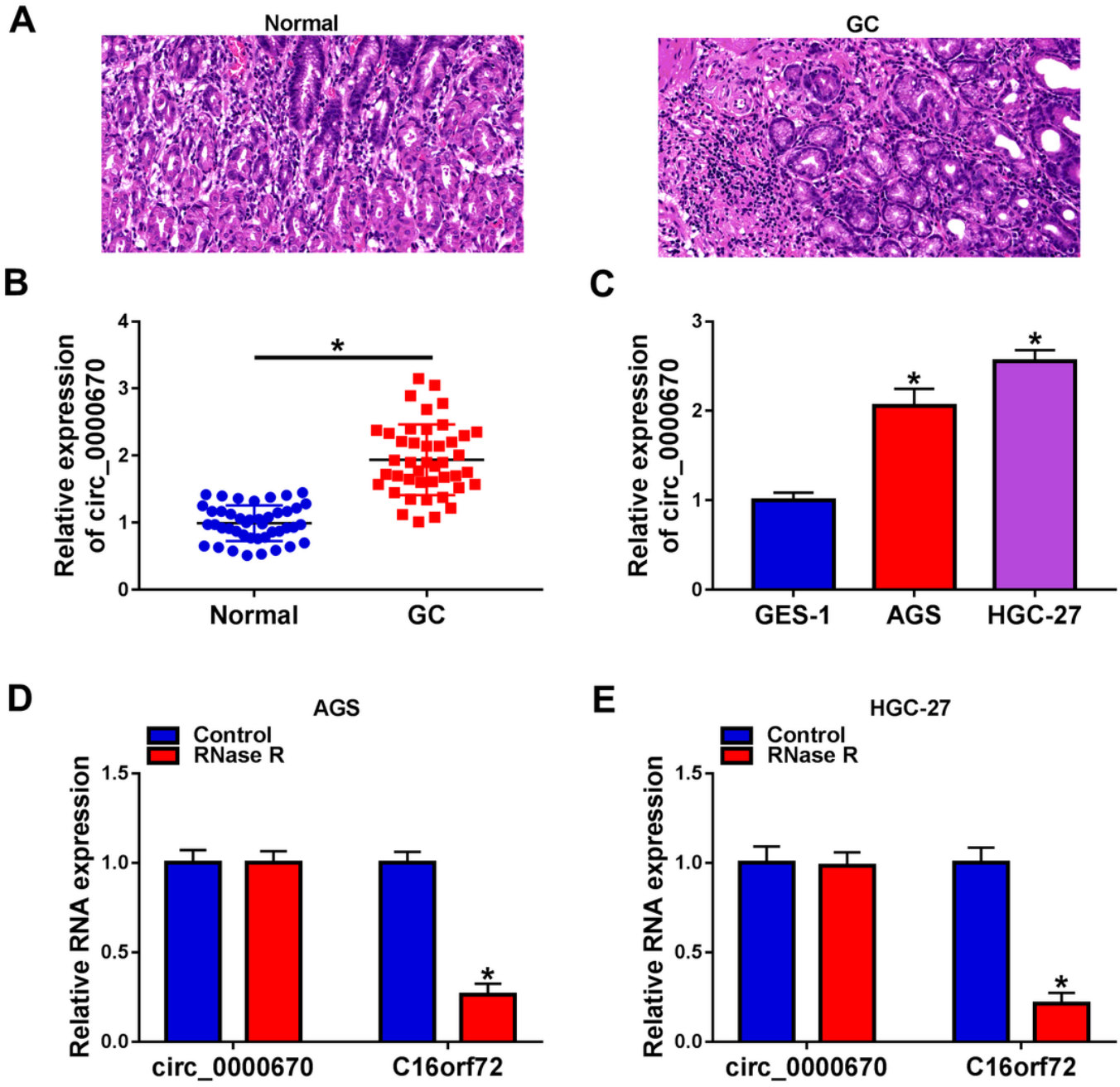

Figure 1

The expression of circ_0000670 was increased in GC tissues and cells. (A) H&E staining assay was conducted to differentiate GC tissues and adjacent normal tissues. **(B)** Circ_0000670 expression in tumor tissues (n=43) and normal paracancer tissues (n=43) was detected by qRT-PCR. **(C)** The expression of circ_0000670 in two GC cell lines (AGS and HGC-27) and a normal gastric epithelial cell line GES-1 was measured by qRT-PCR. **(D and E)** QRT-PCR was used for the abundance of circ_0000670 and C16orf72 in AGS and HGC-27 cells treated with RNase R. **P*<0.05. All cellular experiments were independently repeated three times, and the data were presented in the format of "mean± standard deviation".

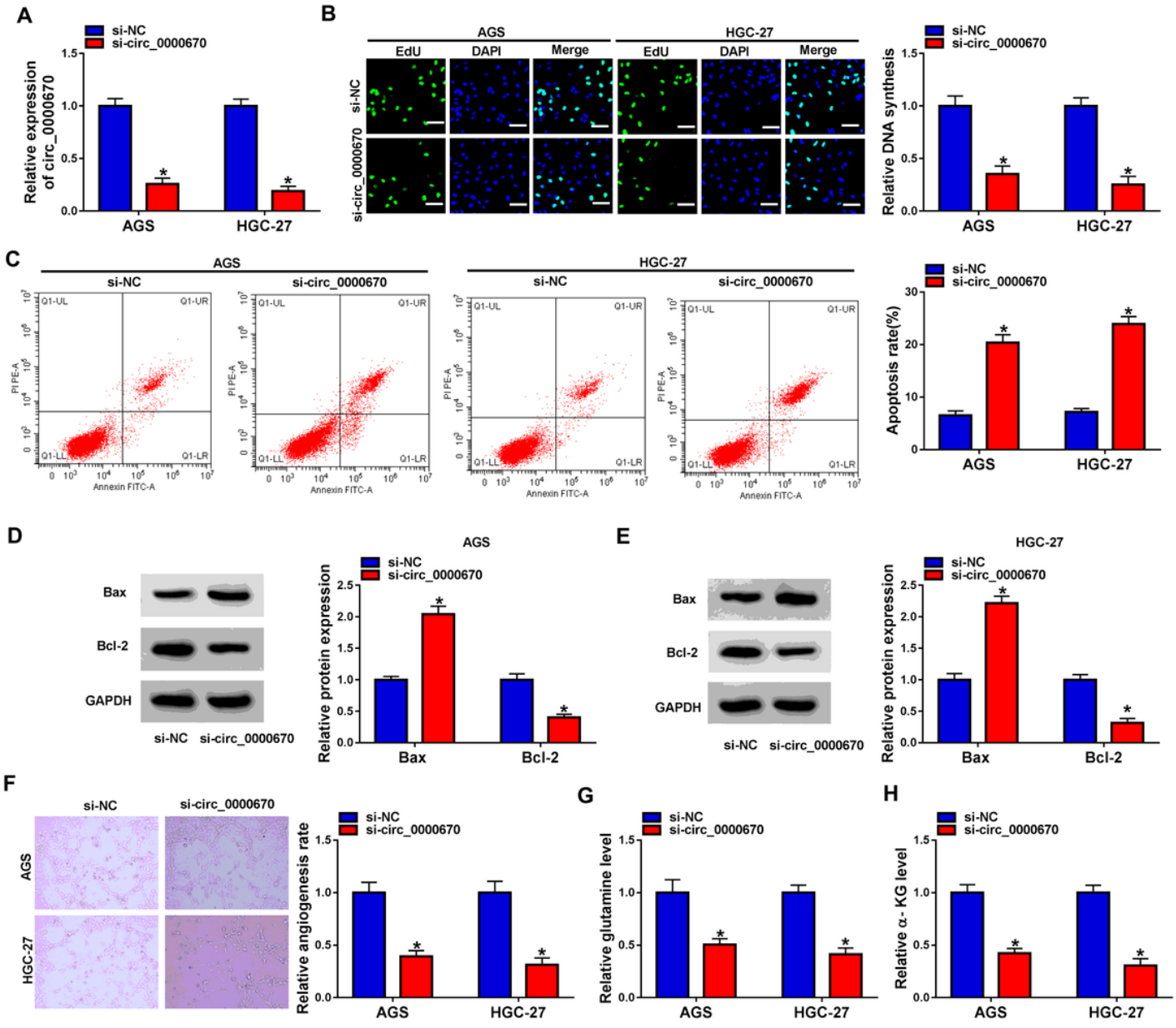

Figure 2

Circ_0000670 knockdown suppressed cell proliferation in GC cells. (A) QRT-PCR was performed to detect the inhibitory efficiency of si-circ_0000670 in AGS and HGC-27 cells. **(B)** The proliferation ability of AGS and HGC-27 cells after si-circ_0000670 transfection was analyzed by EdU assay. **(C)** Flow cytometry was conducted to evaluate the effect of si-circ_0000670 on cell apoptosis. **(D and E)** Western blot assay was used to detect the protein expression of Bax and Bcl-2 in AGS and HGC-27 cells. **(F)** The angiogenesis assay was used to measure the angiogenesis in AGS and HGC-27 cells after transfected with si-circ_0000670. **(G and H)** The effects of circ_0000670 knockdown on glutamine metabolism were evaluated by the levels of glutamine and α-KG. **P*<0.05. All cellular experiments were independently repeated three times, and the data were presented in the format of “mean± standard deviation”.

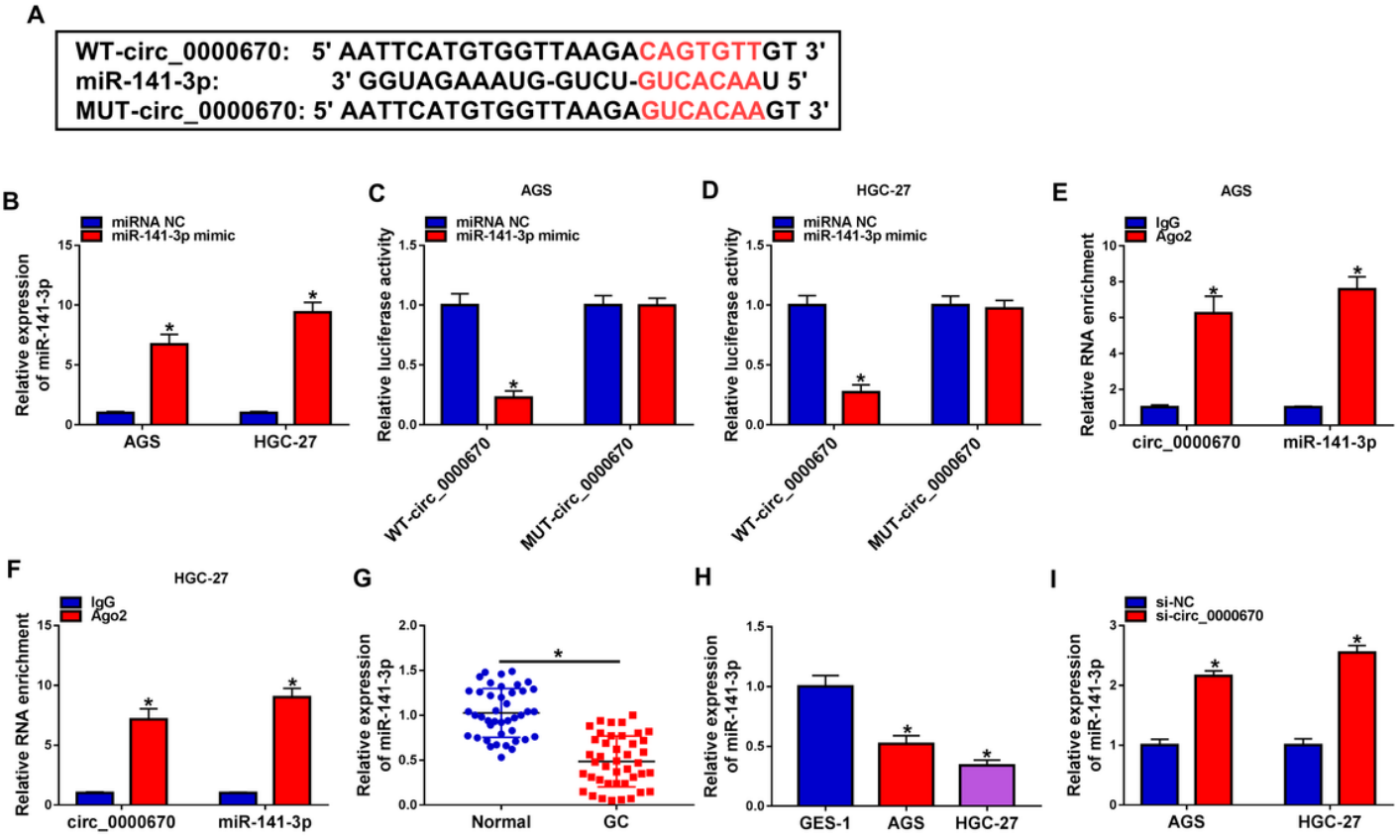

Figure 3

MiR-141-3p was targeted by circ_0000670. (A) The binding sequence between circ_0000670 and miR-141-3p was predicted by circBank. **(B)** The expression of miR-141-3p in GC cells after miR-141-3p mimic transfection was measured by qRT-PCR. **(C and D)** The luciferase activities in each groups were detected with dual-luciferase reporter assay. **(E and F)** The enrichment of circ_0000670 and miR-141-3p in AGS and HGC-27 cells was detected with RIP assay. **(G and H)** The expression of miR-141-3p in GC tissues and cells was detected by qRT-PCR. **(I)** The effect of circ_0000670 down-regulation on the expression of miR-141-3p in AGS and HGC-27 cells was analyzed by qRT-PCR. **P*<0.05. All cellular experiments were independently repeated three times, and the data were presented in the format of "mean± standard deviation".

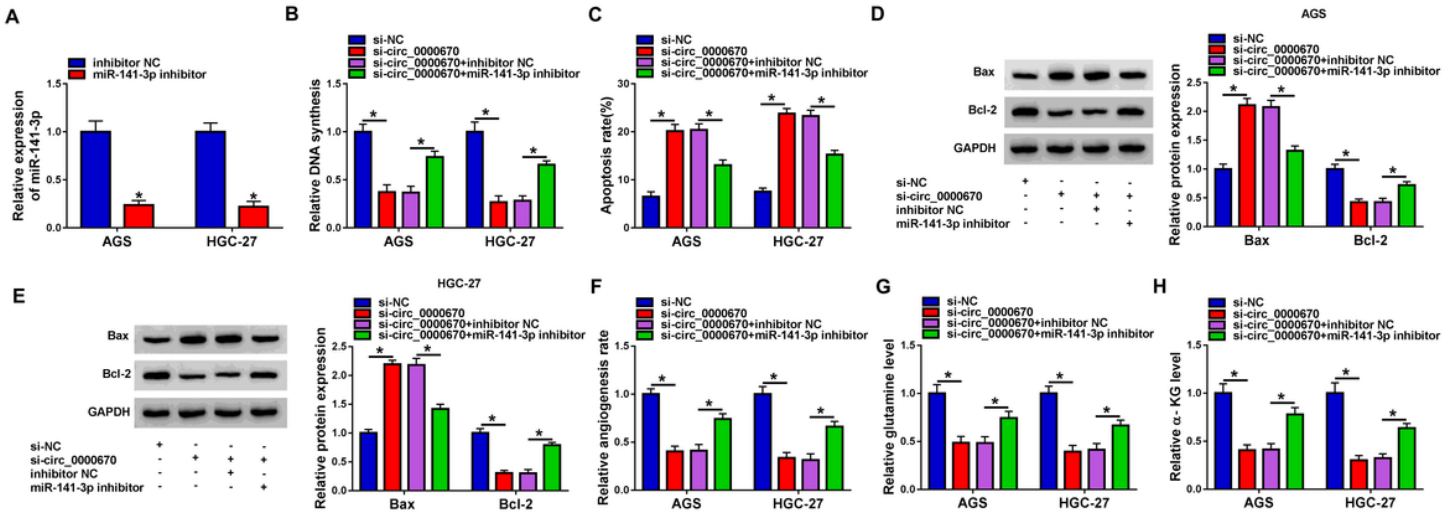

Figure 4

Down-regulation of miR-141-3p reversed the effects of si-circ_0000670 on AGS and HGC-27 cells. (A) The expression of miR-141-3p was measured by qRT-PCR after transfection with inhibitor NC and miR-141-3p inhibitor in AGS and HGC-27 cells. **(B)** The effect of si-circ_0000670 and miR-141-3p inhibitor on the proliferation of GC cells was analyzed by EdU assay. **(C)** Flow cytometry was conducted to analyze the effect of si-circ_0000670 and miR-141-3p inhibitor on the apoptosis of GC cells. **(D and E)** Western blot assay was performed to measure the protein levels of Bax and Bcl-2 in transfected GC cells. **(F)** The angiogenesis assay was conducted to analyze the angiogenesis ability of transfected GC cells. **(G and H)** The effect of si-circ_0000670 and miR-141-3p inhibitor on the glutamine metabolism of GC cells was evaluated by measuring the levels of glutamine and α-KG. **P*<0.05. All cellular experiments were independently repeated three times, and the data were presented in the format of “mean± standard deviation”.

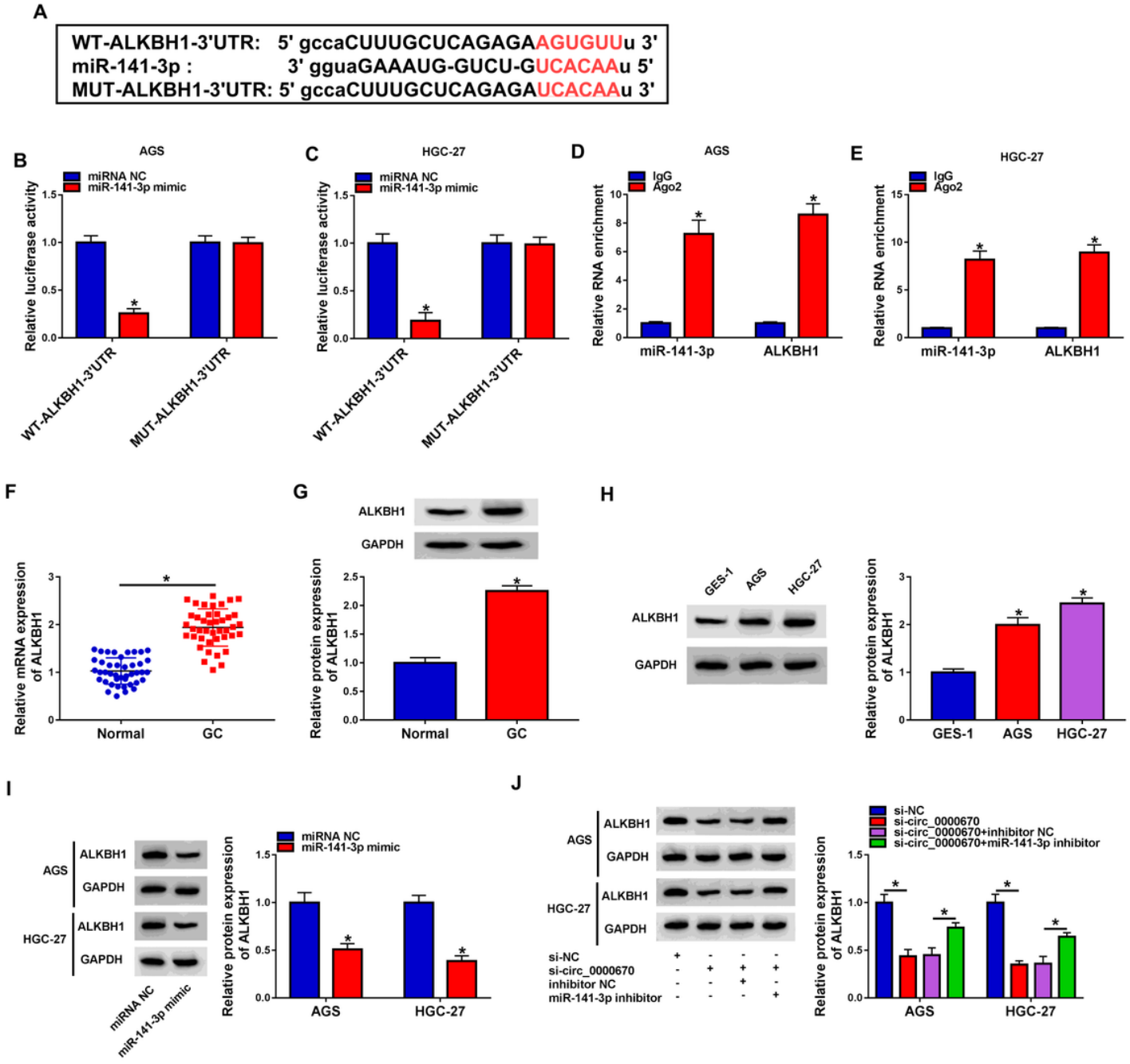

Figure 5

ALKBH1 was bound by miR-141-3p. (A) Target sites of miR-141-3p in ALKBH1 were analyzed by Starbase. **(B and C)** The combination between miR-141-3p and ALKBH1 was verified by dual-luciferase reporter assay. **(D and E)** The interaction between miR-141-3p and ALKBH1 was confirmed by RIP assay. **(F and G)** The mRNA and protein expression of ALKBH1 in GC tissues and adjacent normal tissues was analyzed by qRT-PCR and western blot assay. **(H)** The protein level of ALKBH1 in two GC cell lines (AGS and HGC-27) and a normal gastric epithelial cell line GES-1 was determined by western blot assay. **(I)** Effects of miR-141-3p overexpression on ALKBH1 expression in AGS and HGC-27 cells were analyzed by western blot assay. **(J)** Western blot assay was conducted to detect the protein expression of ALKBH1 in GC cells transfected with si-circ_0000670 alone or together with miR-141-3p inhibitor. *P<0.05. All cellular

experiments were independently repeated three times, and the data were presented in the format of “mean± standard deviation”.

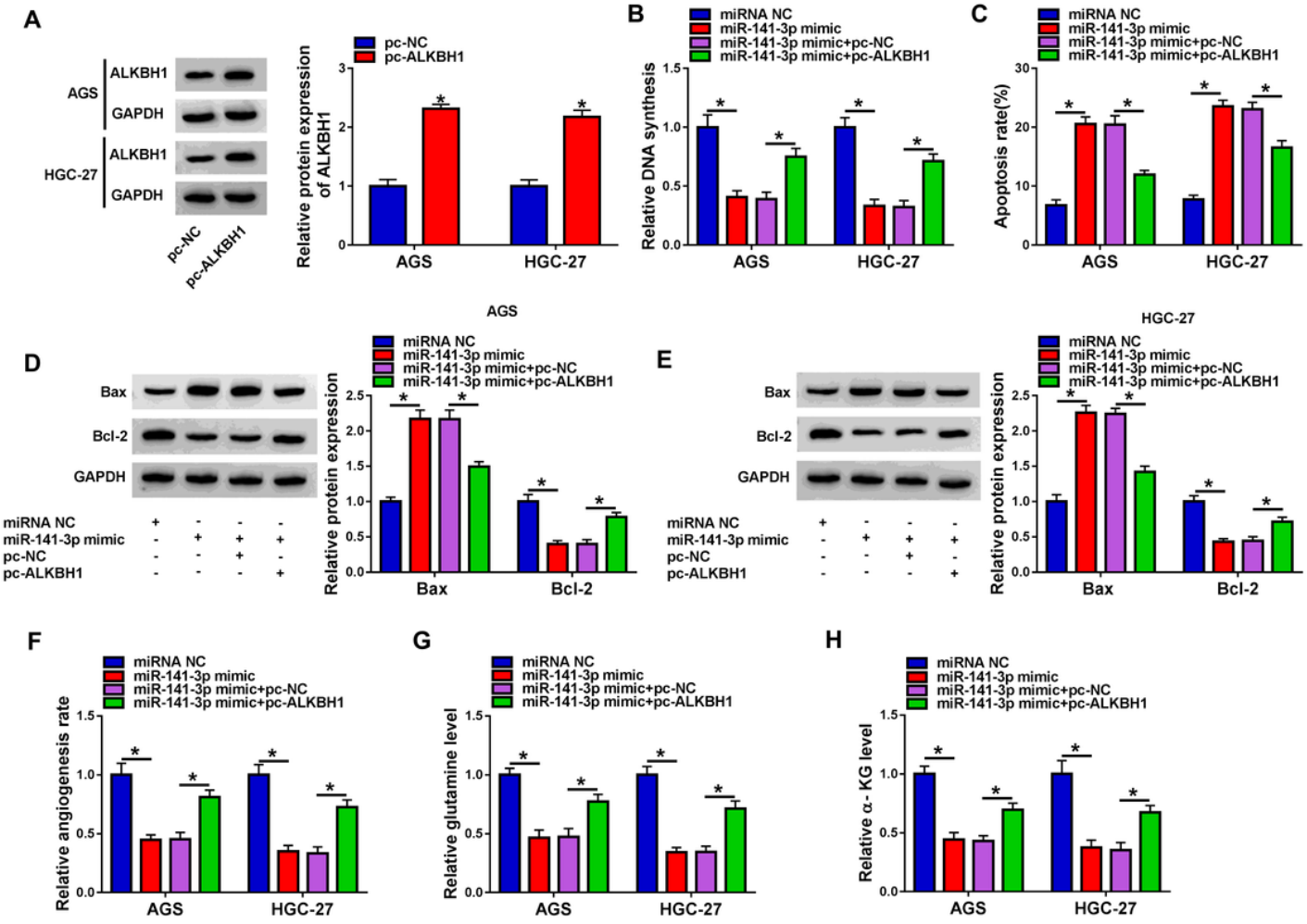

Figure 6

ALKBH1 overexpression overturned the effects of miR-141-3p mimic on the progression ofAGS and HGC-27 cells. (A) The overexpression efficiency of pc-ALKBH1 in AGS and HGC-27 cells was analyzed by qRT-PCR. **(B)** The proliferation of transfected GC cells was analyzed by EdU assay. **(C)** The apoptosis rate of transfected GC cells was assessed by flow cytometry. **(D and E)** Western blot assay was conducted to measure the protein expression of Bax and Bcl-2 in transfected GC cells. **(F)** The tube formation ability of transfected GC cells was analyzed by the angiogenesis assay. **(G and H)** The glutamine metabolism of transfected GC cells was analyzed by detecting the levels of glutamine and α-KG. *P<0.05. All cellular experiments were independently repeated three times, and the data were presented in the format of “mean± standard deviation”.

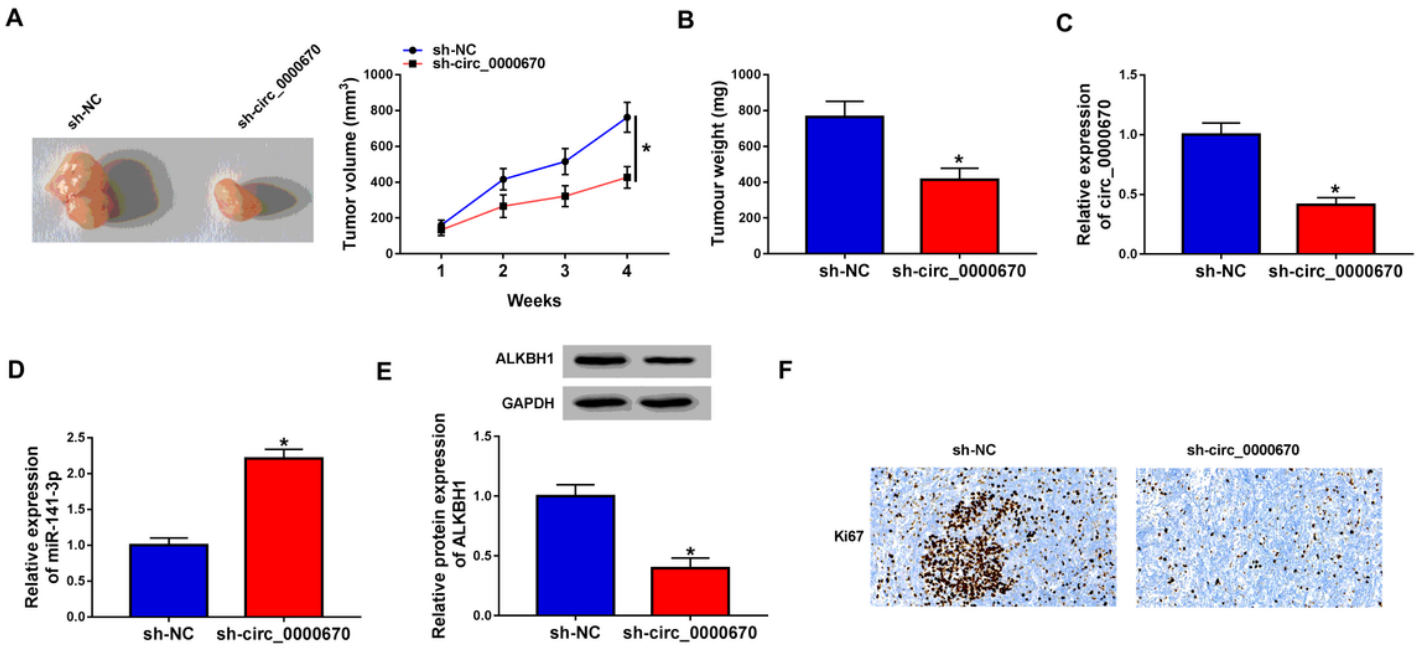

Figure 7

Circ_0000670 knockdown inhibited the tumor growth of GC *in vivo*. (A) The tumor volume was measured every week. **(B)** Tumor weight was detected after 4-week inoculation. **(C to E)** The levels of circ_0000670, miR-141-3p and ALKBH1 protein were examined in each group by qRT-PCR and western blot. **(F)** The level of Ki67 in mouse tissues were detected by IHC assay. **P*<0.05.

Supplementary Files

This is a list of supplementary files associated with this preprint. Click to download.

- file.docx